Cell Reports, Volume *35*

Supplemental information

Divergent clonal differentiation trajectories establish CD8$^+$ memory T cell heterogeneity during acute viral infections in humans

Jeff E. Mold, Laurent Modolo, Joanna Hård, Margherita Zamboni, Anton J.M. Larsson, Moa Stenudd, Carl-Johan Eriksson, Ghislain Durif, Patrik L. Ståhl, Erik Borgström, Simone Picelli, Björn Reinius, Rickard Sandberg, Pedro Réu, Carlos Talavera-Lopez, Björn Andersson, Kim Blom, Johan K. Sandberg, Franck Picard, Jakob Michaëlsson, and Jonas Frisén

Figure S1

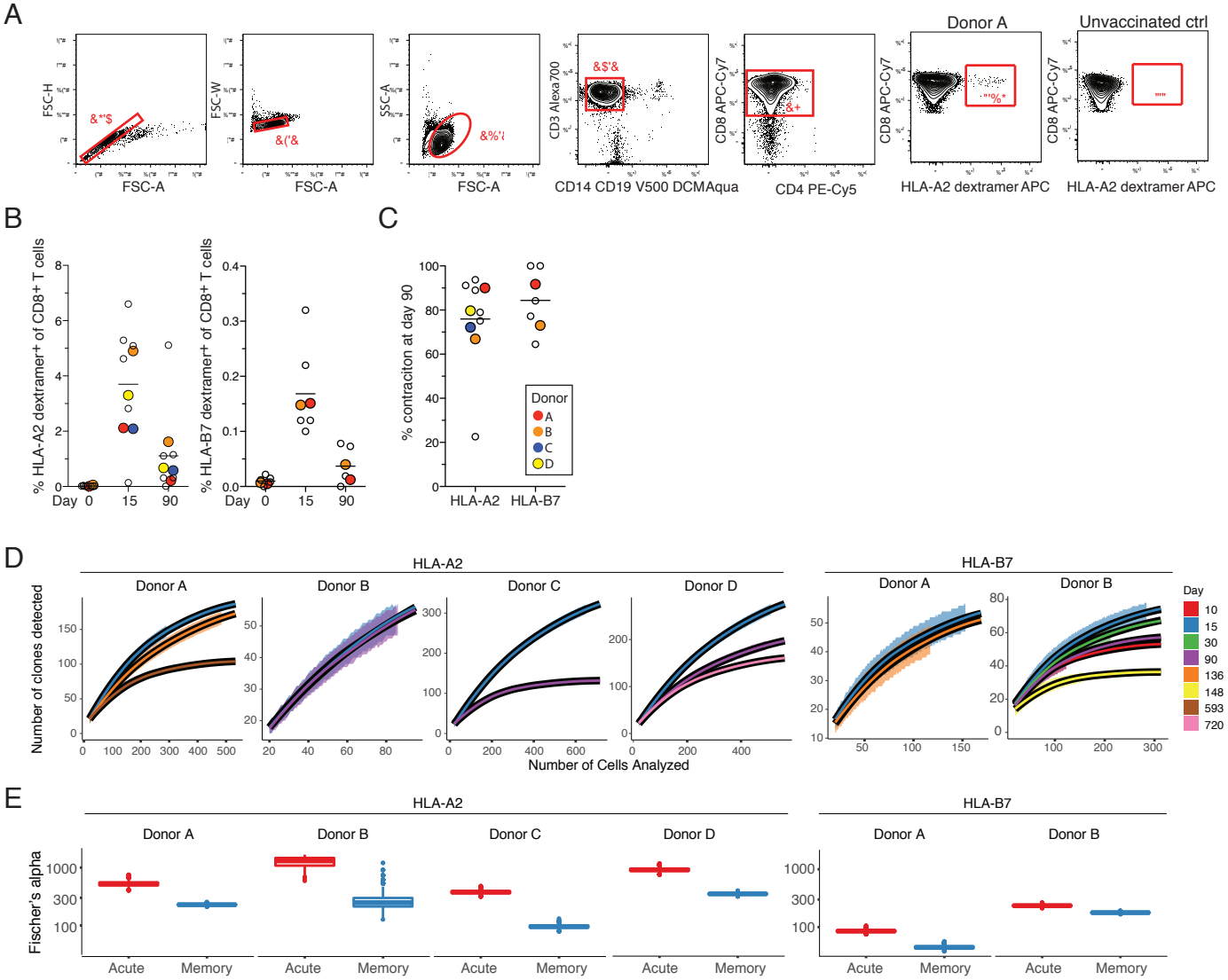

Figure S1: Gating strategy and dynamics of YFV-specific CD8$^+$ T cell responses and clonal diversity (Related to Figures 1, 3): (**A**) Sort strategy for isolating single live CD14$^-$CD19$^-$CD8$^+$Dextramer$^+$ T cells for DNA or RNAseq (Donor A shown). (**B**) Frequencies of YFV-specific HLA-A2/NS4B (left) and HLA-B7/NS5 (right) CD8$^+$ T cell responses at days 0, 15, and 90 after vaccination and (**C**) percent contraction of YFV-specific HLA-A2/NS4B and HLA-B7/NS5 CD8$^+$ T cell responses from day 15 today 90 after vaccination. Colored circles represent donors A-D included in this study. Frequency data for all donors except donors A and B was sourced from Blom et al. (**D**) Bootstrap analysis measuring the number of clones detected in a given sample by sampling a given number of cells from each antigen/timepoint with replacement (donor A-D). 1000 samples were drawn for each cell number starting at n=20 cells and increasing to the maximum number of cells for a given donor/antigen/timepoint combination, and total number of clones identified for each draw was determined. Smooth black line represents Loess regression of bootstrapped number of detected clones for each dataset and colored ribbonsrepresent 90% confidence interval for each dataset relative to number of cells sampled. (**E**) Fischer's-a index, a scale independent indicator of population diversity, for T cells from the acute (≤30 days) or memory (≥90 days) phase for each donor/antigen. 10.000 bootstrap calculations were used with the lowest number of cells present in either early or late group for each dataset. Box plots show Fischer's-a index for all tests. 3-way ANOVA was used to test whether there was a significant drop in diversity between acute and memory phase, controlling for donor and antigen. On average Fischer's-a index dropped from 270 at acute phase to 195 at memory phase ($p>0.001$).

-

s

Figure S2

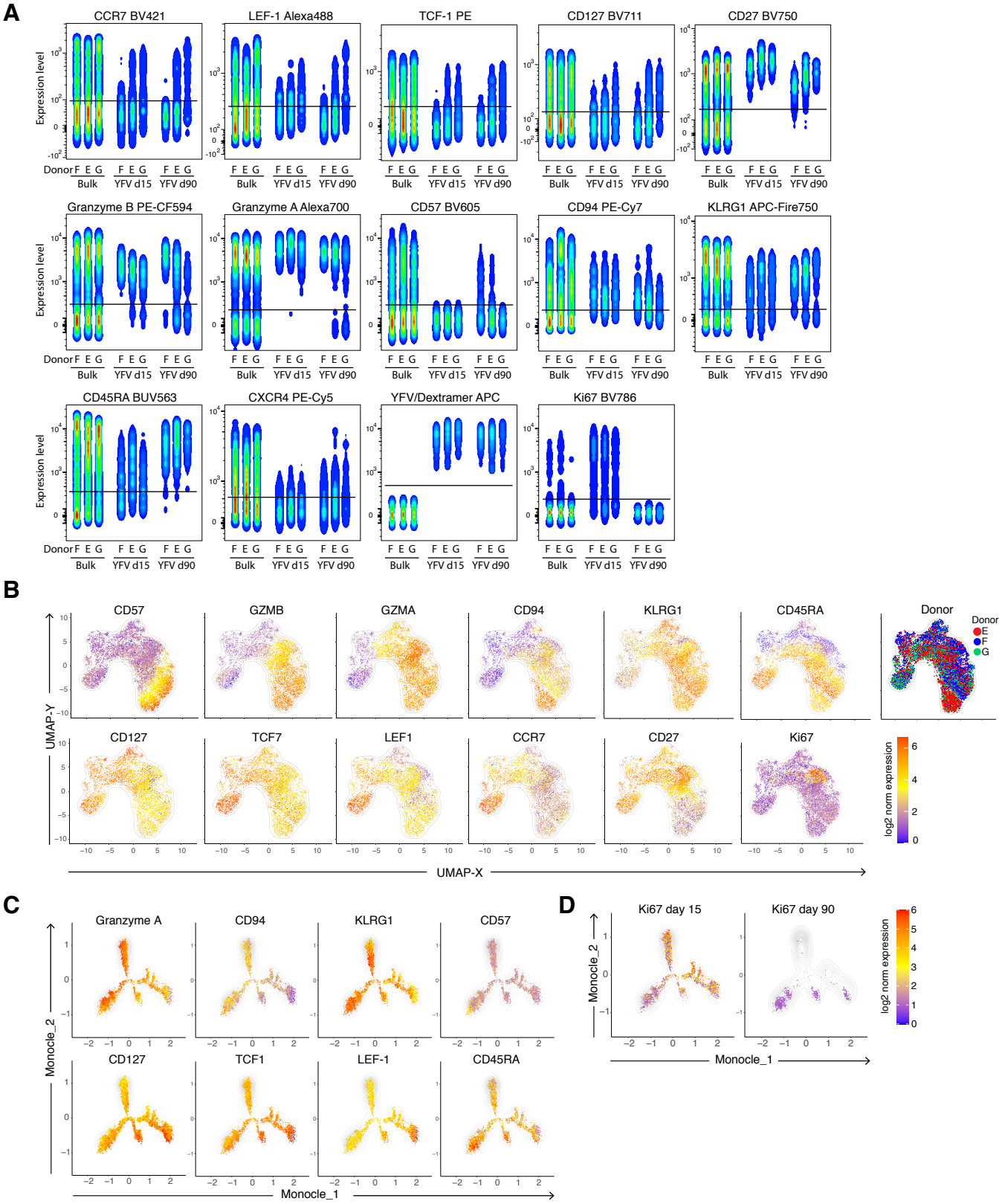

Figure S2: Protein expression by YFV-specific and bulk CD8$^+$ T cells (Related to Figure 2):
(**A**) Protein expression by bulk and YFV-specific CD8$^+$ T cells at day 15 and 90 analyzed by multicolor flow cytometry in 3 donors (donors F, E, and G). (**B**) Expression of indicated proteins in UMAP of bulk CD8$^+$ T cells corresponding to UMAPs for YFV-specific CD8$^+$ T cells in Figure 2A. (**C**) Protein expression for the indicated markers within the Monocle projection for YFV-specific HLA-A2/NS4B- and HLA-B7/NS5-dextramer$^+$ CD8$^+$ T cells from donor E at day 15 and 90 combined. (**D**) Expression of Ki67 at day 15 (left) and day 90 (right) in YFV-specific CD8+ T cells (donor E) within the Monocle projection. Color scales depicts log2 normalized expression values for each protein.

Figure S3

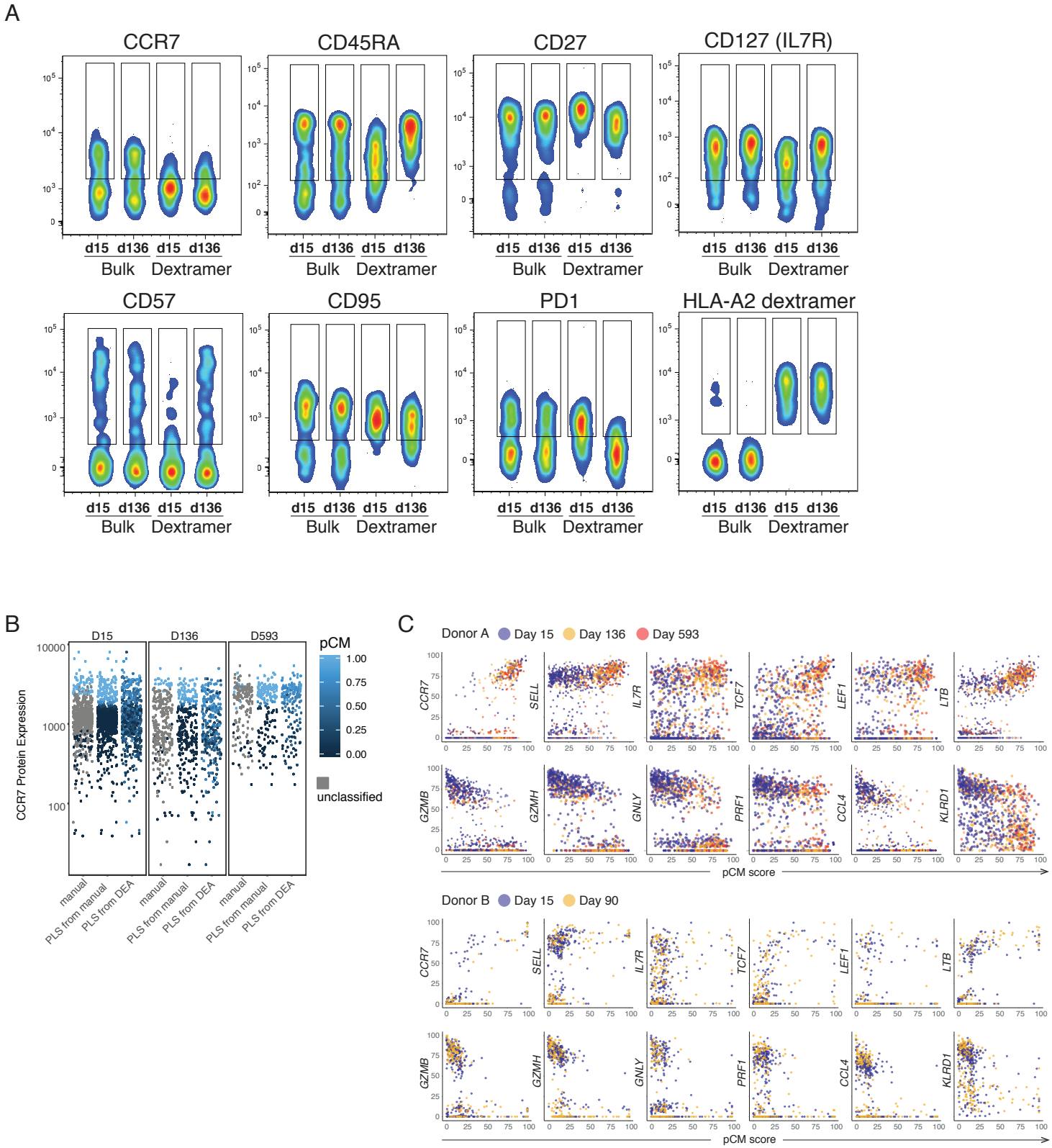

Figure S3: Partial least squares classification of YFV-specific CD8$^+$ T cells (Related to Figure 3):
(**A**) Cell surface phenotype of bulk and YFV-specific CD8$^+$ T cells at day 15 and day 136 from donor A with antibody panel used for index-sorting. CD8$^+$ T cells were enriched by negative-selection using MACS beads and stained with HLA-A2 or HLA-B7 dextramers in combination with the indicated markers, in addition to CD3, CD8, CD14, CD19 and a live/dead marker. Live CD3$^+$CD8$^+$ cells are shown for bulk and CD3$^+$CD8$^+$Dextramer$^+$ cells are shown for YFV-specific CD8$^+$ T cells. (**B**) PLS scoring of single cells relative to CCR7 protein expression at each timepoint for donor A. Single cells were identified to train a partial least squares (PLS) classification as described previously (Durif et al, 2018). First a PLS is trained on manually identified CCR7$^+$ and CCR7$^-$ cells at each timepoint to classify all cells according to similarity based on a small subset of known $T_{CM/SCM}$ and $T_{EM/EMRA}$ markers. Differential expression is then performed on putative $T_{CM/SCM}$ and $T_{EM/EMRA}$ cells according to the initial classification and a second PLS is performed according to patterns of gene expression identified across these cell types to generate a pCM score. (**C**) Classification of single YFV-specific CD8$^+$ T cells in donor A and Donor B based on pCM Score. Typical $T_{CM/SCM}$ and $T_{EM/EMRA}$ genes expressed relative to pCM score in single YFV-specific CD8$^+$ T cells in donor A (upper panels) and donor B (lower panels). Day after vaccination is indicated by color.

Figure S4

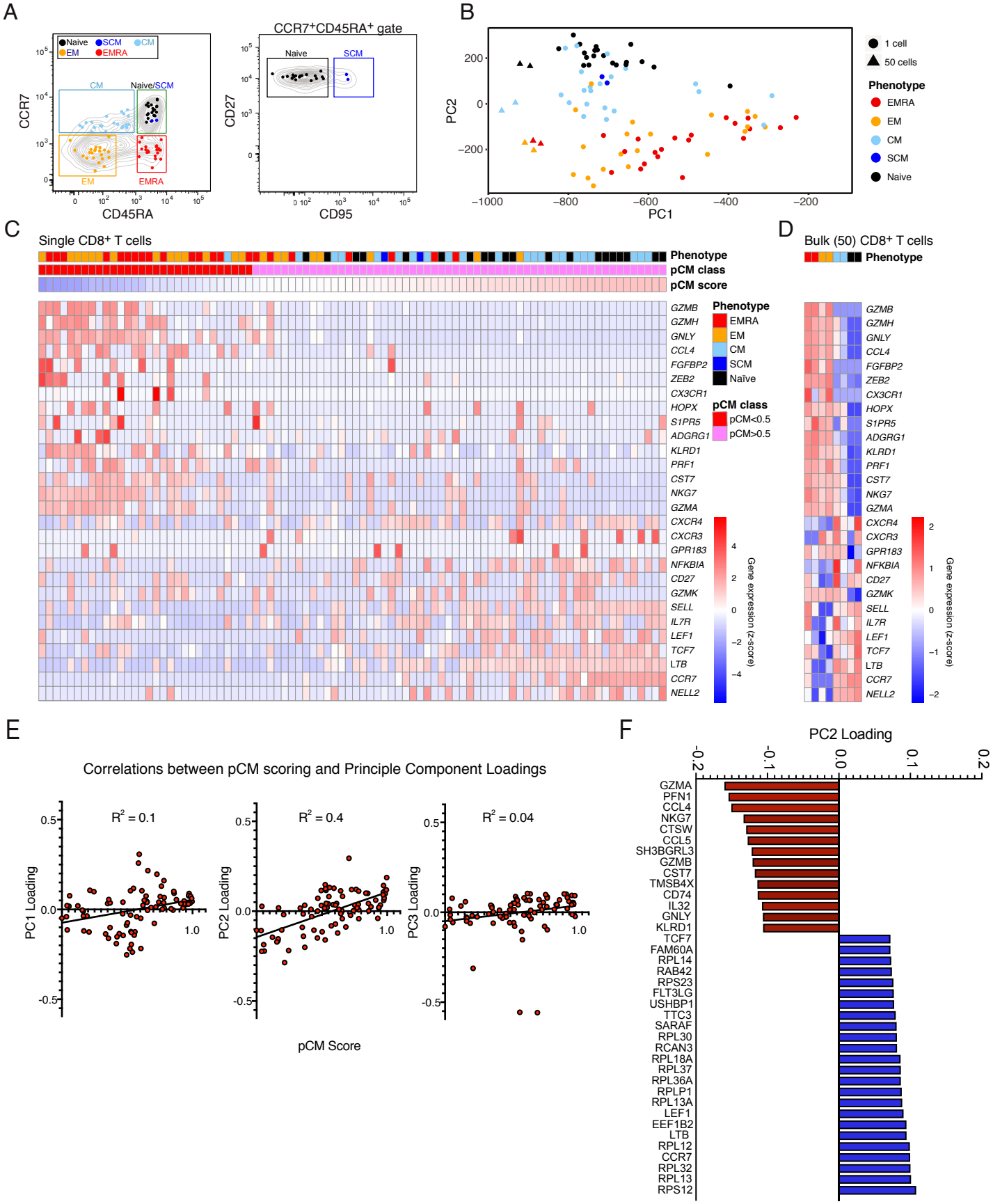

Figure S4: Validation of pCM score using sorted CD8$^+$ T cells (Related to Figure 3):
(**A**) Sorting strategy to identify CD8$^+$ T cell types in blood. Naïve (black), T_{CM} (light blue), T_{EM} (orange) and T_{EMRA} (red) in bulk CD8$^+$ T cells. Two T_{SCM} were identified among CD45RA$^+$CCR7$^+$ cells based on expression of CD95 (dark blue). Single cells and bulk (50 cells) RNAseq was performed on each of the naïve, T_{CM}, T_{EM} and T_{EMRA} populations. (**B**) Principle component analysis of single cells and bulk T cells analyzed by RNAseq. PC2 separates subsets, while PC1 primarily identifies differences in number of unique genes detected. (**C**) Combined RNAseq analysis and PLS allows classification of pCM score despite sparse expression of genes typically associated with $T_{SCM/CM}$ and $T_{EM/EMRA}$ cells. Heatmap shows expression of selected genes for single CD8$^+$ T cells ordered according to pCM score. Phenotype by cell surface protein expression and pCM class is indicated at top of heatmap. (**D**) Gene expression data for bulk (50 cells) sequencing of each population.
(**E**) pCM score versus PC1, PC2, and PC3. (F) Enrichment of typical $T_{EM/EMRA}$ and $T_{SCM/CM}$ genes in PC2 loadings.

Figure S5

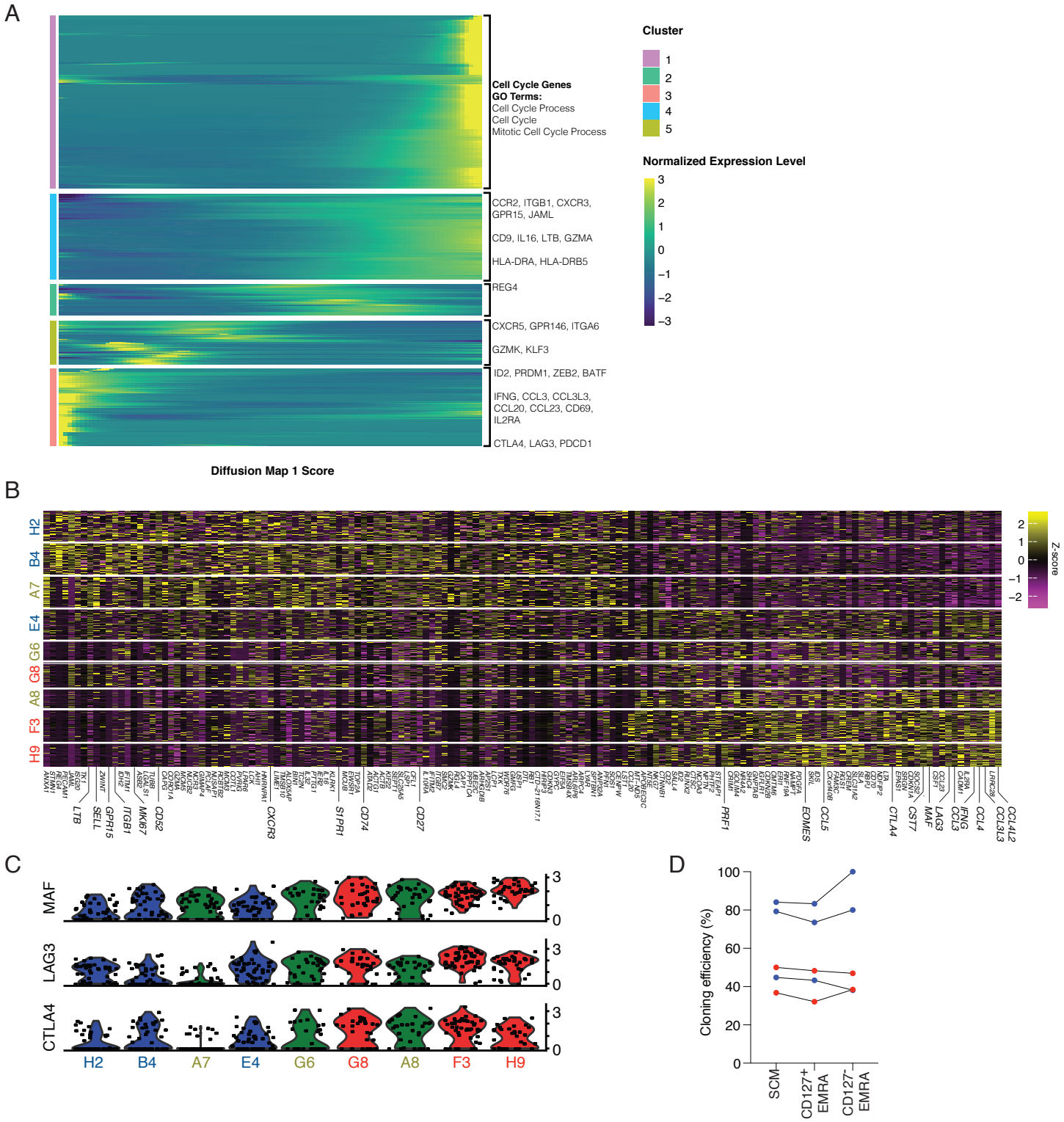

Figure S5: Genes associated with diffusion map score 1 and founder cell-related DEGs (Related to Figure 4 and 5): (**A**) Heatmap depicting genes associated with Diffusion Map 1 (DM1) score used in Figure 4F. Genes labeled for each cluster include known T cell functional genes associated with cytotoxicity or cell migration and effector functions. GO terms for cluster 1 depicted since most genes in this cluster were cell cycle related. (**B**) Differentially expressed genes in progeny from T_{SCM} and T_{EMRA} founder cells. Heatmap depicting differentially expressed genes (padj<0.05) between progeny of single YFV-specific $CD8^+$ T_{SCM} or T_{EMRA} founder cells. (**C**) Increased expression of inhibitory receptors in T_{EMRA}-derived progeny. Expression of MAF, LAG3, and CTLA4 in progeny of single YFV-specific $CD8^+$ T_{SCM} or T_{EMRA} founder cells. Scaled gene expression values are shown. (**D**) Similar cloning efficiency across $CD8^+$ T cell subsets. Percentage of wells seeded with the indicated $CD8^+$ T cell founder cell type that had detectable YFV-specific $CD8^+$ T cell progeny. Results from 5 independent experiments are shown.

Figure S6

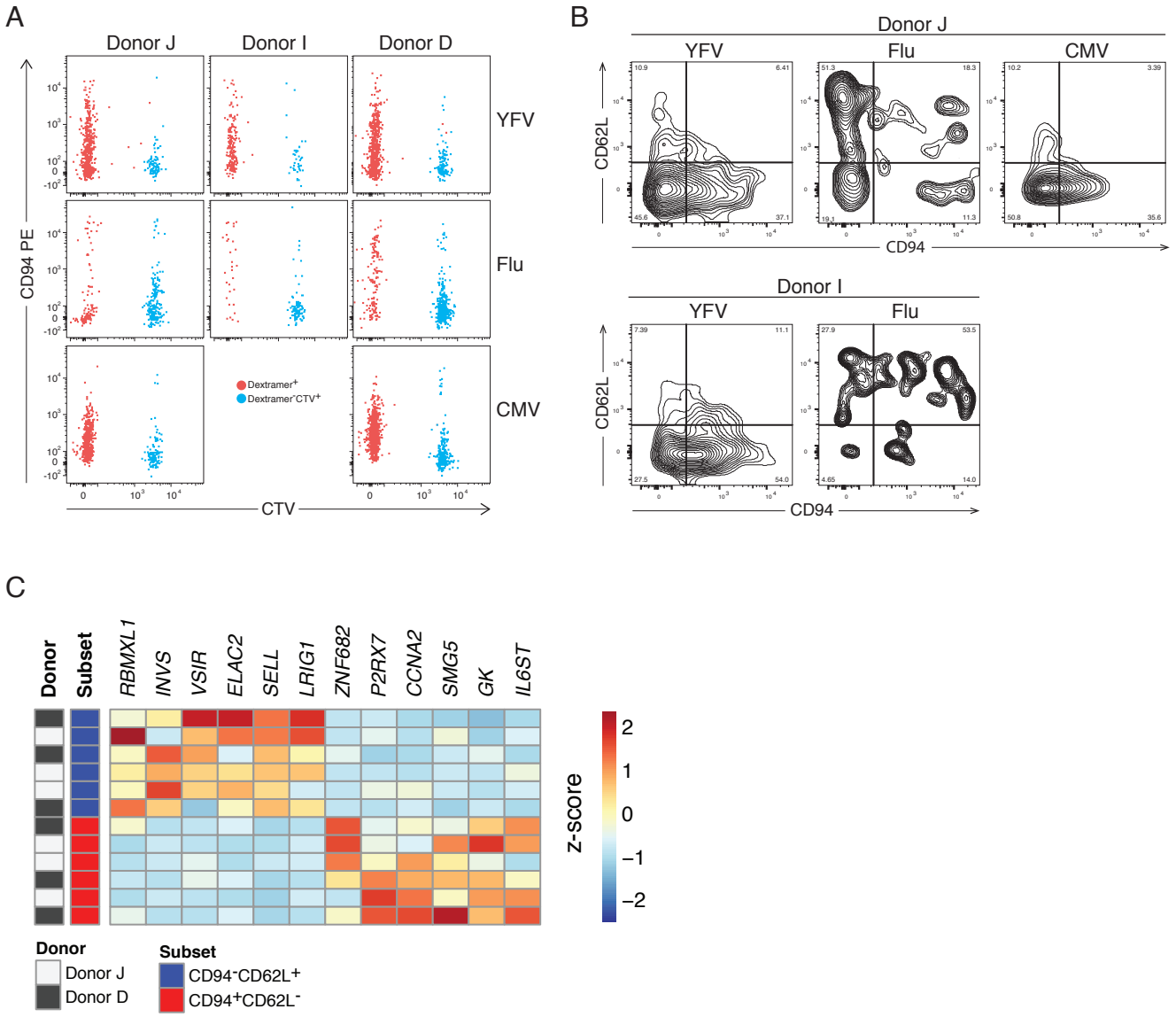

Figure S6: Characterisation of expanded YFV-, Flu, and CMV-specific CD8$^+$ T cells (Related to Figure 6): (**A**) Proliferation of YFV-, Flu-, and CMV-specific CD8$^+$ T cells. CD8$^+$ T cell proliferation analyzed by cell trace violet (CTV) dilution after 2 weeks of stimulation with YFV NS4B, Flu M1, or CMV pp65 HLA-A2-restricted epitopes in 3 donors. Red depicts virus-specific CD8$^+$ T cells (HLA-A2-dextramer$^+$ cells), and blue depicts CTV$^+$ dextramer$^-$ CD8$^+$ T cells. (**B**) Expression of CD62L and CD94 on YFV-, Flu-, and CMV-specific CD8$^+$ T cells after 2 weeks of stimulation. HLA-A2-dextramer$^+$ live CD8$^+$ T cells from donor I and donor J are shown. (**C**) Differentially expressed genes between CD62L$^+$CD94$^-$ and CD62L$^-$CD94$^+$ CMV-specific CD8$^+$ T cells.